Targeted Cardiac Overexpression of A20 Improves Left Ventricular Performance and Reduces Compensatory Hypertrophy After Myocardial Infarction

Hong-Liang Li, MD, PhD*; Ming-Lei Zhuo, BSc*; Dong Wang, MD*; Ai-Bing Wang, PhD; Hua Cai, PhD; Li-Hong Sun, MSc; Qinglin Yang, PhD; Yue Huang, PhD; Yu-Sheng Wei, PhD; Peter P. Liu, MD; De-Pei Liu, PhD; Chih-Chuan Liang, PhD

Background—A20 was originally characterized as a tumor necrosis factor–inducible gene in human umbilical vein endothelial cells. As an inhibitor of nuclear factor-κB signaling, A20 protects against apoptosis, inflammation, and cardiac hypertrophy. In the present study, we tested the hypothesis that cardiac-specific overexpression of A20 could protect the heart from myocardial infarction.

Methods and Results—We investigated the role of constitutive human A20 expression in acute myocardial infarction using a transgenic model. Transgenic mice containing the human A20 gene under the control of the α-myosin heavy chain promoter were constructed. Myocardial infarction was produced by coronary ligation in A20 transgenic mice and control animals. The extent of infarction was then quantified by 2-dimensional and M-mode echocardiography and by molecular and pathological analyses of heart samples in infarct and remote heart regions 7 days after myocardial infarction. Constitutive overexpression of A20 in the murine heart resulted in attenuated infarct size and improved cardiac function 7 days after myocardial infarction. Significantly, we found a decrease in nuclear factor-κB signaling and apoptosis, as well as proinflammatory response, cardiac remodeling, and interstitial fibrosis, in noninfarct regions in the hearts of constitutive A20-expressing animals compared with control animals.

Conclusions—Cardiac-specific overexpression of A20 improves cardiac function and inhibits cardiac remodeling, apoptosis, inflammation, and fibrosis after acute myocardial infarction. (***Circulation*. 2007;115:1885-1894.)**

Key Words: apoptosis ■ cardiovascular diseases ■ fibrosis ■ gene therapy ■ hypertrophy ■ inflammation ■ remodeling

Cardiovascular disease accounts for nearly 40% of all deaths annually in developed countries. In particular, acute myocardial infarction (MI) represents an enormous clinical challenge as loss of myocardium. After the acute phase of MI, a chronic phase of ventricular remodeling occurs. This phase is maladaptive and associated with persistent cardiomyocyte apoptosis, inflammation, wall thinning, fibrosis, ventricular chamber enlargement, and hypertrophy, which contribute to the development of depressed cardiac function, clinical heart failure, and increased mortality.[1–3] Intervention to minimize these progressive changes is highly desirable to reduce the incidence and severity of congestive heart failure that may develop after MI. Therefore, it is of critical importance to explore the mechanisms for maladaptation and to develop therapeutic strategies that are effective in inhibiting this deleterious process.

Editorial p 1827
Clinical Perspective p 1894

One way to achieve successful attenuation of the deleterious process after MI is to overexpress proteins in the heart that are usually protective against cardiac inflammation, apoptosis, fibrosis, and hypertrophy.[4] The zinc finger protein A20 represents such a candidate for genetic engineering of heart. A20, originally identified as a tumor necrosis factor (TNF)–responsive gene in endothelial cells, is expressed in multiple cell types in response to a variety of stimuli that

Received August 5, 2006; accepted December 29, 2006.

From the National Laboratory of Medical Molecular Biology (H.-L.L, M.-L.Z., A.-B.W., L.-H.S., Y.H., Y.-S.W., D.-P.L., C.-C.L) and Department of Anatomy, Histology, and Embryology (D.W.), Institute of Basic Medical Sciences, Chinese Academy of Medical Sciences and Peking Union Medical College, Beijing, China; Section of Cardiology (H.C.), Department of Medicine, Division of Biological Sciences and Pritzker School of Medicine, University of Chicago, Chicago, Ill; Cardiovascular Research Institute (Q.Y.), Morehouse School of Medicine, Atlanta, Ga; and Heart and Stroke/Richard Lewar Centre of Excellence (P.P.L). University Health Network, University of Toronto, Toronto, Ontario, Canada.

*The first 3 authors contributed equally to this work.

The online-only Data Supplement, consisting of Methods, is available with this article at http://circ.ahajournals.org/cgi/content/full/CIRCULATIONAHA.106.656835/DC1.

Correspondence to De-Pei Liu, PhD, National Laboratory of Medical Molecular Biology, Institute of Basic Medical Sciences, Chinese Academy of Medical Sciences and Peking Union Medical College, Beijing, 100005, PR China. E-mail liudp@pumc.edu.cn

Circulation **is available at http://www.circulationaha.org** **DOI: 10.1161/CIRCULATIONAHA.106.656835**

activate nuclear factor (NF)-κB.[5,6] Recent studies showed that A20 expression protects different types of cells against TNF-mediated apoptosis.[5,6] In addition, we showed recently that A20 expression protects against oxidative low-density lipoprotein–induced macrophage apoptosis.[7]

Cook and colleagues[8] reported that A20 is dynamically regulated during acute biomechanical stress in the heart and functions to attenuate cardiac hypertrophy. Indeed, early work also demonstrated that NF-κB activity is significantly upregulated within minutes after MI and can be increased further after reperfusion.[9] Despite the potentially significant roles of A20 in attenuating NF-κB–dependent apoptotic, inflammatory, and hypertrophic signaling in general, it has remained unclear whether A20 is involved in post-MI myocardial adaptation and remodeling and whether a targeted myocardial overexpression of A20 is cardioprotective. Thus, in the present study, we generated a transgenic (TG) mouse model in which high levels of A20 were selectively overexpressed in the myocardium. We compared TG mice with wild-type (WT) controls for their post-MI cardiac function at physiological and molecular levels. Intriguingly, we found that TG mice had markedly improved functional recovery, decreased inflammation, reduced apoptosis, and retarded ventricular remodeling, as well as diminished interstitial fibrosis, when examined on day 7 after acute MI. These findings clearly demonstrate that cardiac-specific overexpression of A20 may be a useful strategy for protection against post-MI cardiac remodeling and maladaptation.

Methods

Animals and Surgical Procedures

All protocols were approved by institutional guidelines. All surgeries and subsequent analyses were performed by researchers blinded to genotype. Details on the generation of TG mice (Laboratory Animal Center, Academy of Military Science, Beijing, China) expressing a cardiac-specific human A20 and surgical procedures are given in the expanded Methods section in the online Data Supplement.

Blood Pressure and Echocardiography

Heart rate and systolic blood pressure was measured by tail-cuff plethysmography (BP-2000 System, Visitech Systems, Apex, NC).[10] Echocardiography was performed by SONOS 5500 ultrasound (Philips Electronics, Amsterdam, the Netherlands) with a 15-MHz linear-array ultrasound transducer. Details are provided in the expanded Methods section in the online Data Supplement.

Cardiac Morphology and Histomorphometric Analysis

Details on cardiac morphology and histomorphometric analysis are provided in the expanded Methods section in the online Data Supplement.

Measurement of Myeloperoxidase Activity

Myeloperoxidase, an enzyme specific for neutrophils, was determined in cardiac tissue by the method described previously.[11]

Measurement of Plasma Levels of Cytokines and Ventricular Atrial and Brain Natriuretic Protein Concentrations

Plasma levels of interleukin (IL)-1β, monocyte chemoattractant protein (MCP)-1, IL-6, and TNF-α were evaluated by use of commercially available solid-phase sandwich ELISA kits (R&D Systems, Minneapolis, Minn) using the protocol recommended by the manufacturer. Ventricular atrial natriuretic protein (ANP) and brain natriuretic protein (BNP) concentrations were measured by specific radioimmunoassays as reported previously.[12]

Determination of Apoptosis

Cell death by apoptosis was evaluated after measuring oligonucleosomal DNA fragments by a TUNEL assay performed in sections with use of the CardiaoTACS In Situ Apoptosis Detection Kit (R&D Systems) according to the manufacturer's recommendations and by a DNA laddering assay as described previously.[7]

Northern and Western Blot Analyses

Details on Northern and Western blot analyses are provided in the expanded Methods section in the online Data Supplement.

Electrophoretic Mobility Shift Assay and IκB Kinase Assay

Details on electrophoretic mobility shift assay and IκB kinase (IKK) assay are provided in the expanded Methods section in the online Data Supplement.

Statistical Analysis

All values are expressed as mean±SEM. The differences in the data simply between 2 groups were determined by Student *t* test. Comparisons between groups on Western blotting data were assessed by 1-way ANOVA, followed by Bonferroni post hoc test. Values of $P<0.05$ were considered statistically significant.

The authors had full access to and take full responsibility for the integrity of the data. All authors have read and agree to the manuscript as written.

Results

Characterization of Cardiac-Specific Human A20 TG mice

To assess the effect of constitutive human A20 expression on myocardial, we generated TG mice lines with full-length human A20 cDNA under the control of the α-myosin heavy chain promoter (Figure 1A). Four lines of TG mice were confirmed by polymerase chain reaction. These lines were viable and fertile, and there were no detectable differences in cardiac size and structure between TG and WT mice either macroscopically or microscopically. We analyzed A20 protein levels in various tissues by Western blot analysis using anti-A20 antibody. We found a robust expression of human A20 protein in the heart, but it was not detected in the other organs (Figure 1B). Among 4 established lines of TG mice, 1 line that expressed the highest level of human A20 protein in the heart was used for further experiments (Figure 1C). Northern blot results showed that the expression level of the mouse A20 mRNA was not modified or downregulated by the expression of human A20 gene (Figure 1D).

A20 Gene Expression in the Heart After Acute MI

We evaluated the expression of A20 in the infarcted heart. Northern blot using probes specific to either human A20 or mouse A20 demonstrated 2 major findings. First, mRNA levels of TG A20 were not affected by MI, and this pattern of expression persisted in hearts for 7 days after infarction. Second, in early infarction (6 hours after coronary ligation), levels of endogenous A20 mRNA significantly increased ($P<0.05$) compared with sham-operated TG mice (Figure 2). By 24 hours after infarction, the levels of mouse A20 mRNA

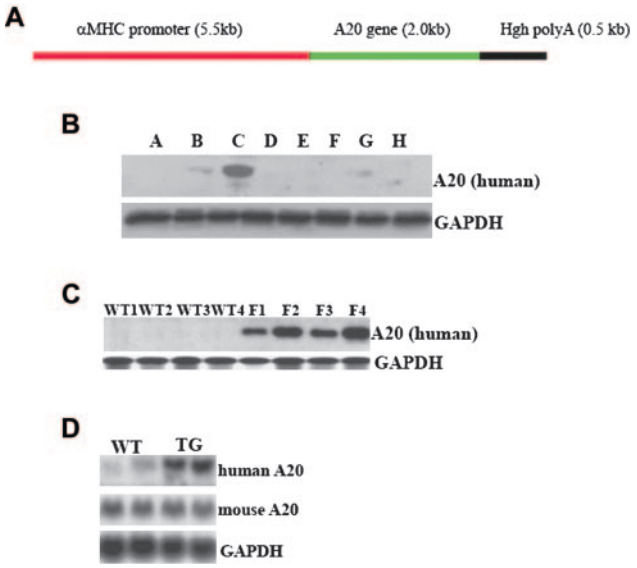

Figure 1. Characterization of human A20 TG mice. A, Diagram of the transgene construct used to generate A20 TG mice. The construct contains the α-myosin heavy chain promoter, full-length human A20 cDNA clone, and human growth hormone polyadenylylation. B, Representative Western blot analysis of human A20 protein from different tissue of TG mice (A, lung; B, brain; C, heart; D, spleen; E, muscle; F, liver; G, kidney; H, testis). C, Representative Western blot analysis of human A20 protein in the heart tissue from 4 lines of both TG and WT mice. D, Northern blot analysis of TG A20 and endogenous A20 mRNA levels in the heart from TG mice.

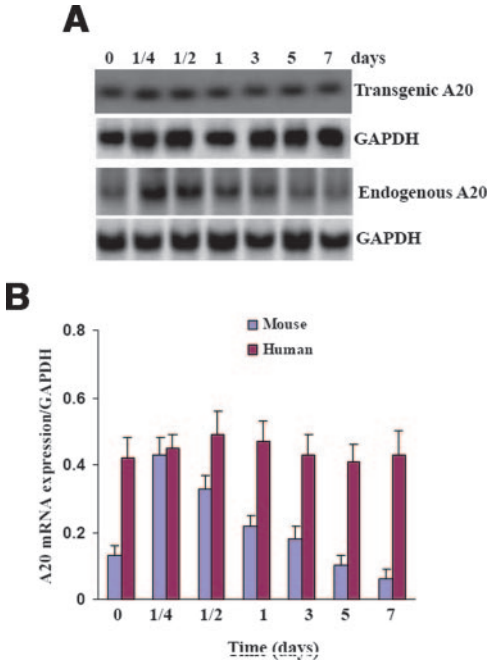

Figure 2. The effect of myocardial infarct on A20 mRNA expression. A, Representative Northern blot analysis of mouse and human A20 mRNA in the heart tissue from TG mice after acute MI at the time points indicated. B, Quantitative analysis of mouse and human A20 mRNA in the heart tissue from TG mice (n=7 for each) after acute MI at the time points indicated. Each assay was done in triplicate. Values are mean±SEM.

were low in infarcted tissue of TG mice. At day 7, mouse A20 mRNA expression was almost not detectable in the infarcted heart.

Survival After Surgery

Of those undergoing left anterior descending artery ligation, 7 mice (4 WT, 3 TG mice) died within 24 hours and were excluded from the study. All sham-operated mice survived surgery and to the end of the observation period. Among left anterior descending artery–ligated mice, there were 13 deaths in WT mice (13 of 29) and 12 deaths in TG mice (12 of 28) at 7 days. Although the survival rate was not different statistically, the rate of ventricular rupture was significantly lower in TG-MI mice (6 of 28) than WT-MI mice (10 of 29). To further investigate the effect of A20 on heart injury mediated by MI, we examined the survival rate at 14 days after MI. The results showed that the survival rate was much higher in TG-MI than WT-MI mice (56.7% versus 37.5%; n=32 for each group; $P<0.05$). No ventricular rupture was observed after 7 days.

Cardiac Performance and Infarct Size After Infarction in A20 TG Mice and Control

We assessed cardiac function 7 days after MI in TG and WT mice by echocardiography. The cardiac functional parameters evaluated by echocardiography 7 days after left anterior descending artery ligation are shown in the Table. There was no significant difference in heart rate and systolic blood pressure among 4 groups of mice. In WT-MI mice, markedly decreased fractional shortening and ejection fraction with dilated left ventricular end-systolic and end-diastolic diameters were seen, corresponding to post-MI failure. In TG-MI mice, much lower left ventricular end-systolic and end-diastolic diameters and much higher fractional shortening and ejection fraction were observed compared with that in

Echocardiographic Characteristics in WT and A20 TG Mice After Sham Operation and MI

	Sham		MI	
	WT	TG	WT	TG
N	13	11	8	8
BW, g	32.1±0.7	31.6±1.2	36.1±1.3*	30.5±0.8*‡
SBP, mm Hg	106±4.7	110±6.3	105.4±2.5	112.5±1.8
HR, bpm	403±21	411±15	409±14.5	418±17
HW/BW, mg/g	5.23±0.12	5.28±0.13	5.98±0.14*	5.32±0.12‡
PWT, mm	2.52±0.14	2.61±0.16	3.16±0.11*	2.82±0.13*
LVEDD, mm	3.52±0.12	3.44±0.13	4.45±0.32†	3.85±0.15‡
LVESD, mm	1.66±0.12	1.72±0.12	3.11±0.13†	2.40±0.11*‡
FS, %	55±4.5	56±3.8	28±3.4†	37.7±3.1†‡
EF, %	62±2.3	58±2.1	38.4±2.7†	43.7±4.6†‡

BW indicates body weight; SBP, systolic blood pressure; HR, heart rate; HW, heart weight; PWT, posterior wall thickness; LVEDD, left ventricular end-diastolic diameter; LVESD, left ventricular end-systolic diameter; FS, fractional shortening; and EF, ejection fraction. All values are mean±SE (n=8 to 13).

*$P<0.05$, †$P<0.001$ vs WT-sham group; ‡$P<0.05$, §$P<0.001$ vs WT-MI group.

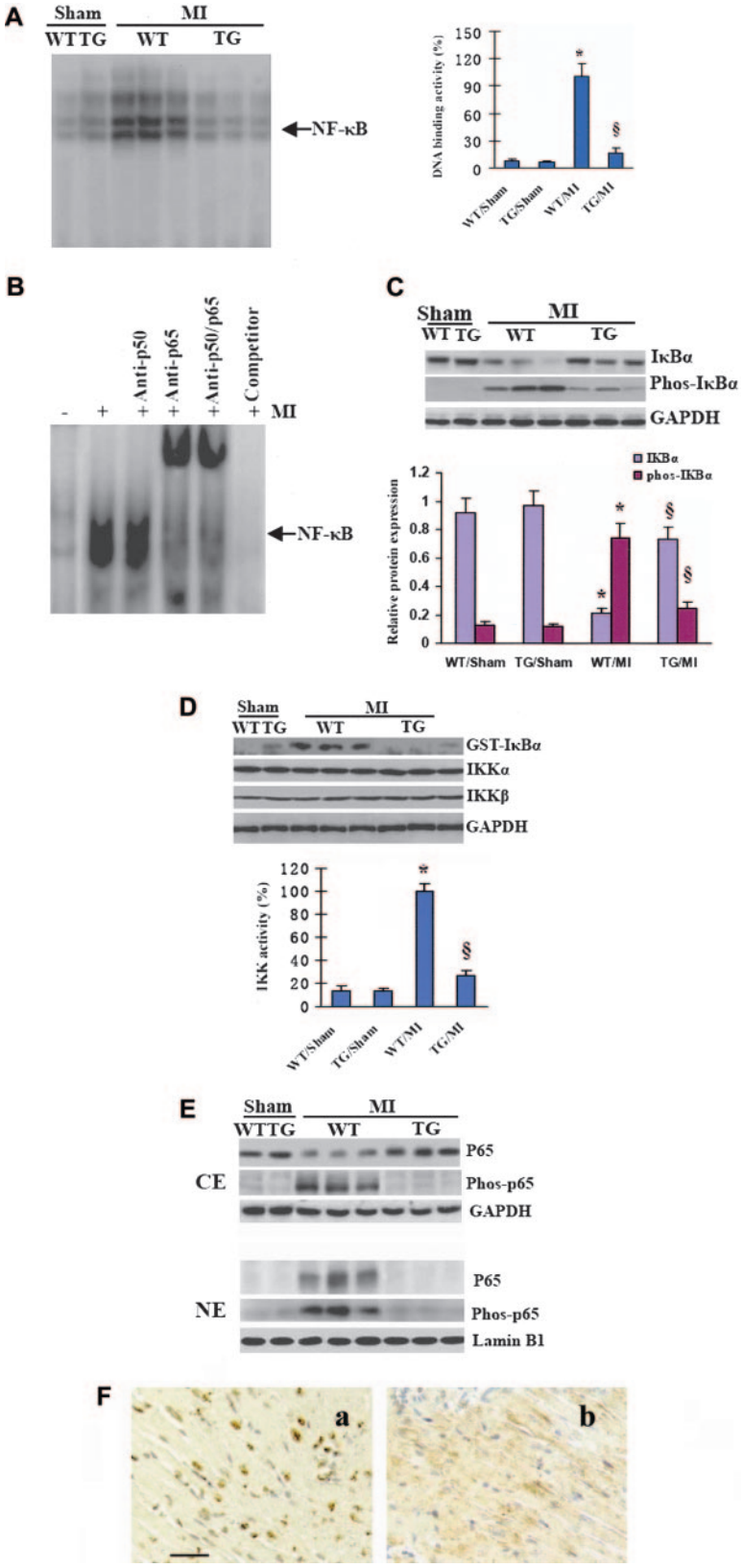

Figure 3. A20 overexpression blocks NF-κB activation induced by MI. A, Left, Representative electrophoretic mobility shift assay of NF-κB activity in myocardium 7 days after MI in 4 groups of animals (n=6 for each). Right, Optical density in region of NF-κB was quantified with the PhosphorImager system. B, NF-κB induced by MI is composed of p65 and p50 subunits. Nuclear extracts (NEs) from MI or sham-WT hearts were incubated with the indicated antibodies, unlabeled NF-κB oligo-probe, and then assayed for NF-κB activation by electrophoretic mobility shift assay. A20 is specific in inhibiting NF-κB. C, Western blot analysis of IκBα degradation and phosphorylation in cytoplasmic extracts (CEs) of myocardium obtained from 4 groups of animals (n=6). Top, Representative blots; bottom, quantitative results. D, Top, CEs were assayed for IKK by the immunocomplex kinase assay (top) and for IKK-α (middle) and IKK-β (bottom) protein by Western blot analysis as described in Methods. Bottom, Quantitative results. E, A20 inhibited p65 phosphorylation and translocation induced by MI. Western blot analysis of p65 translocation and phosphorylation in CE and NE of myocardium obtained from 4 groups of animals (n=6). CE and NE fractions were prepared and analyzed by Western blot with anti-p65, anti-GAPDH, or anti–lamin B1. Anti–lamin B1 was used as a loading control for the amount of NE loaded; anti-GAPDH was used as a control for the amount of CE loaded. F, Tissue sections from WT and TG mice were immunostained with antibodies against p65 (a, WT-MI; b, TG-MI; scale bar=30 μm). Each assay was done in triplicate. Values are mean±SEM *$P<0.01$ vs WT-sham values; §$P<0.01$ vs WT-MI values.

WT-MI mice. Sham-operated animals had no evidence of myocardial dysfunction as assessed by echocardiography. Infarct size determined by morphometric analysis 7 days after MI was calculated as the total area occupied by scar divided by the total ventricular area. The average infarct size was 37.6±2.4% in WT-MI mice but only 26.4±1.8% in TG-MI mice ($P<0.01$). We further assessed the acute infarct size at 24 hours after MI and found no significant difference between WT-MI and TG-MI mice (33.1±2.7% versus 30.6±1.1%; n=16 for each group).

A20 Overexpression Blocks NF-κB Signaling

As shown in Figure 3A, 7 days of MI evidently increased the activation of NF-κB in the myocardium in WT mice, while it was abolished in TG mice regardless of MI. The specificity of NF-κB DNA binding activity was confirmed by supershift assays (Figure 3B). To determine the molecular mechanisms by which A20 blocks NF-κB activation in vivo, we first analyzed IκBα phosphorylation and IKK activation processing, indicators of activation of the canonical NF-κB pathways, 7 days after MI. Heart lysates were prepared, and Western blot analyses were performed with appropriate antibodies. We detected IκBα phosphorylation and IκBα degradation clearly 7 days after MI in WT mice. However, IκBα phosphorylation and IκBα degradation were significantly impaired in TG mice (Figure 3C). Because phosphorylation of IκBα is mediated through IKKβ, these results suggested that A20 may inhibit IKKβ activation. Indeed, as shown in Figure 3D, in immune-complex kinase assays, MI activated IKKβ in WT mice, and A20 overexpression completely suppressed the activation. Under these conditions, A20 had no effect on IKKα and IKKβ protein levels. The translocation of p65 to the nucleus is important to NF-κB activation. Therefore, we also tested the effect of A20 on MI-induced phosphorylation and translocation of p65. As shown in Figure 3E, MI induced the phosphorylation and nuclear translocation of p65 determined by Western blot analysis 7 days after MI in WT mice. However, such phosphorylation and nuclear translocation were abrogated in TG mice. The membranes were reprobed with anti–lamin B1 as a control for the amount of nuclear protein loaded. To further confirm the translocation of p65, heart sections of WT and TG mice were analyzed by immunostaining. Similar to the Western blot data, p65 stain–positive cells were found to be highly expressed in the nucleus of cardiomyocytes of WT-MI mice but far less in TG-MI mice (Figure 3F).

A20 Overexpression Impaired Proinflammatory Response Induced by MI

To determine whether expression of A20 prevents the inflammatory responses in the hearts, the cellular infiltrates were characterized by immunohistochemical analyses; 7/4 is a marker that labels mainly neutrophils, Mac-1 is expressed mainly on monocytes/macrophages, and Mac-3 is expressed specifically by activated macrophages.[13] The number of 7/4-, Mac-1–, and Mac-3–positive cells was clearly increased in the hearts of WT mice 7 days after MI compared with the age-matched WT-sham mice (Figure 4A through 4C). In contrast, the number of 7/4-, Mac-1–, and Mac-3–positive cells was greatly decreased in the hearts of TG mice (Figure 4A through 4C). These results show that the increase in the number of neutrophils, macrophages, and activated macrophages was inhibited by the presence of A20. To further quantify the extent of inflammatory cell infiltration, we measured the activity of cardiac myeloperoxidase, an enzyme specific to activated neutrophils. When myocardial myeloperoxidase activity was measured in infarcted tissues 7 days after MI, we found that the activity significantly increased within the infarcted areas of both TG and WT mice but that it was significantly lower in the TG mice (Figure 4D). Our results also showed that TG mice have significantly lower TNF-α, IL-1β, IL-6, and MCP-1 protein expression 7 days after MI compared with WT infarcts (Figure 4E). As a further study, we also

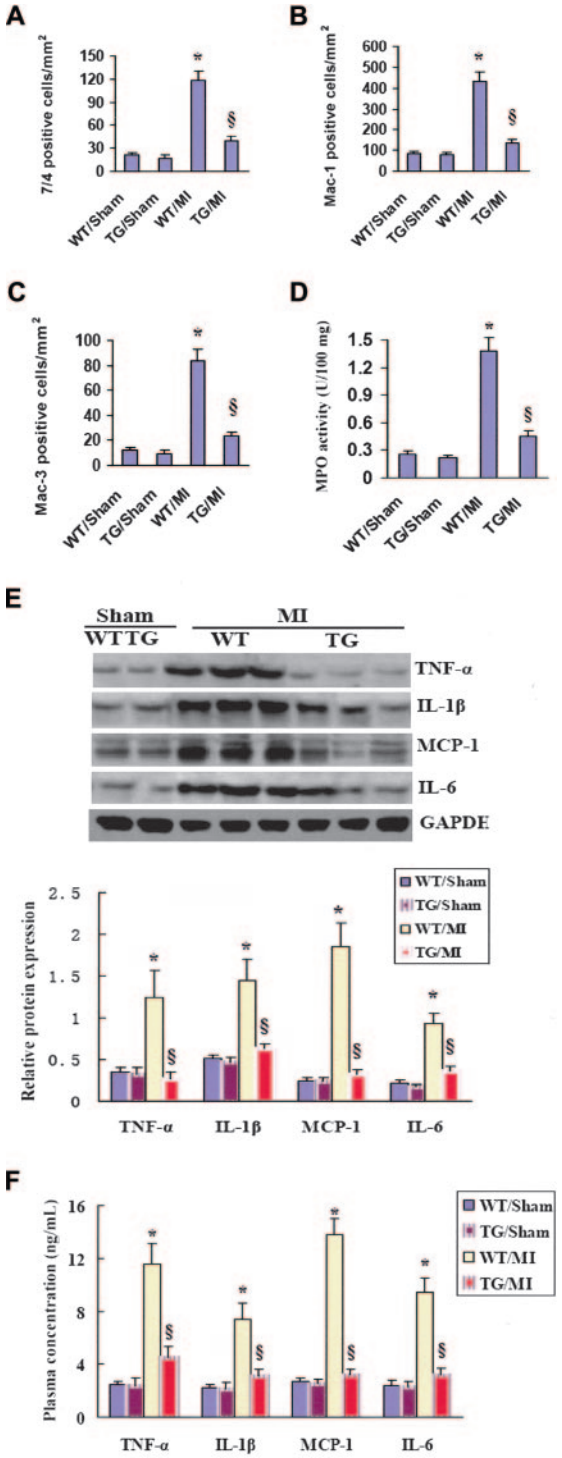

Figure 4. A20 overexpression blocks proinflammatory response induced by myocardial infarct. A–C, Quantitative analysis showed the number of 7/4-, Mac-1–, and Mac-3–positive cells in the hearts of WT and TG mice (n=4). D, Myocardial myeloperoxidase activity in infarcted cardiac tissue samples from TG and WT mice (n=6). Myeloperoxidase activity is expressed as U/100 mg wet tissue weight. E, Western blot analysis of TNF-α, IL-1β, IL-6, and MCP-1 protein expression in myocardium obtained from TG and WT mice (n=6). Top, Representative blots; bottom, quantitative results. F, Inhibition of proinflammatory cytokine production in plasma. Plasma samples were collected from the left ventricle in TG and WT mice 7 days after MI (n=6). Each assay was done in triplicate. Values are mean±SEM. MPO indicates myeloperoxidase.*$P<0.01$ vs WT-sham values; §$P<0.01$ vs WT-MI values.

investigated the concentrations of these proinflammatory cytokines in plasma 7 days after MI. Yet again, we observed an attenuation of levels of TNF-α, IL-1β, IL-6, and MCP-1 in TG-MI mice compared with that in WT-MI mice (Figure 4F).

A20 Overexpression Protects From Apoptosis and Regulated Genes Involved in Apoptosis

To detect apoptosis, DNA ladder and TUNEL assay were performed. DNA ladder appeared faint in the noninfarcted left ventricle from TG-MI mice compared with that from WT-MI mice, suggesting the attenuation of apoptosis by A20 overexpression (Figure 5A). Myocardial tissue sections were stained with TUNEL staining. TUNEL-positive nuclei were rarely seen in control mice, whereas their number increased in the noninfarcted left ventricle from WT-MI mice and was significantly decreased in TG-MI mice (Figure 5B). Thus, both methods demonstrated significant attenuation of apoptosis in TG hearts. To determine whether TG mice are resistant to intrinsic death signals, we first examined caspase-3 and -9 cleavages, as well as cytochrome c and Smac/Diablo release, in TG and WT mice 7 days after MI. As expected, TG mice displayed a significant delay of caspase-3 and caspase-9 cleavages in response to MI. Similarly, A20 overexpression suppressed cytochrome c and Smac/Diablo release induced by MI (Figure 5C). These results indicate that the inhibitory effect of A20 on cardiomyocyte apoptosis is due primarily to blocking of intrinsic death signals. To further elucidate the mechanism of the antiapoptotic effect of A20, we examined whether expression of apoptosis-related genes, including survivin, bcl-2, XIAP, cFLIP, Fas, FasL, and Bax, were changed in TG mice. Western blot analyses revealed that A20 expression preserved the expression of the antiapoptotic proteins survivin, bcl-2, XIAP, and cFLIP and decreased the expression of the proapoptotic proteins Fas, FasL, and Bax (Figure 5D). These results suggest that A20 promotes cardiomyocyte survival, at least in part, through the regulation of apoptosis-related genes expression.

A20 Overexpression Inhibits Left Ventricular Remodeling in Response to MI

Cross-sectional area of cardiac myocytes, an index of cellular hypertrophy, increased in the noninfarcted left ventricle from WT-MI mice and was significantly attenuated in TG-MI mice (Figure 6A). We next examined whether A20 overexpression affects the cardiac expression of hypertrophy-related genes, in which we used ANP and BNP as markers. In WT mice, the expression level of ANP and BNP mRNA and protein increased significantly 7 days after MI compared with that in sham-operated mice (Figure 6B and 6C), indicating that MI induced gene expression, along with the development of cardiac hypertrophy. In TG mice, however, expression levels were significantly lower than in WT mice hearts, suggesting inhibitory effects of A20 on ANP and BNP mRNA and protein expression. We further measured tissue levels of ANP and BNP in the ventricle 7 days after MI by radioimmunoassay. As shown in Figure 6D, before MI, the levels of ventricular ANP and BNP were 11.7±1.8 and 41.5±4.6 ng/g, respectively. Seven days after MI, ventricular ANP and BNP levels were ≈3 times higher

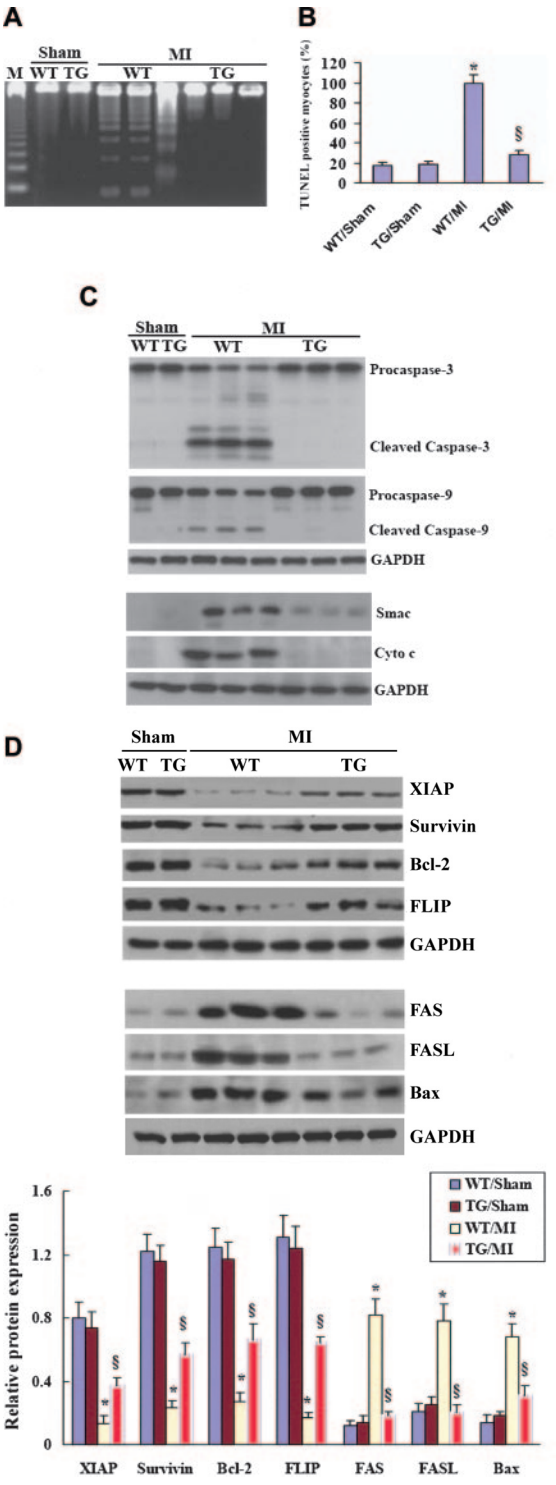

Figure 5. A20 overexpression protects from cardiomyocyte apoptosis induced myocardial infarct. A, DNA ladder indicating apoptosis in genomic left ventricular DNA from 4 groups of animals (n=6 each). B, Quantitative results of the TUNEL-positive number in the hearts of WT and TG mice (n=4). Values are mean±SEM. C, Western blot analysis of caspase-3 and -9 cleavages and cytochrome c and Smac/Diablo release in myocardium obtained from 4 groups of animals (n=6). D, Western blot analysis of survivin, bcl-2, XIAP, cFLIP, Fas, FasL, and Bax protein expression in myocardium obtained from 4 groups of animals (n=6). Top, Representative blots; bottom, quantitative results. Values are mean±SD. *$P<0.01$ vs WT-sham values; §$P<0.01$ vs WT-MI values.

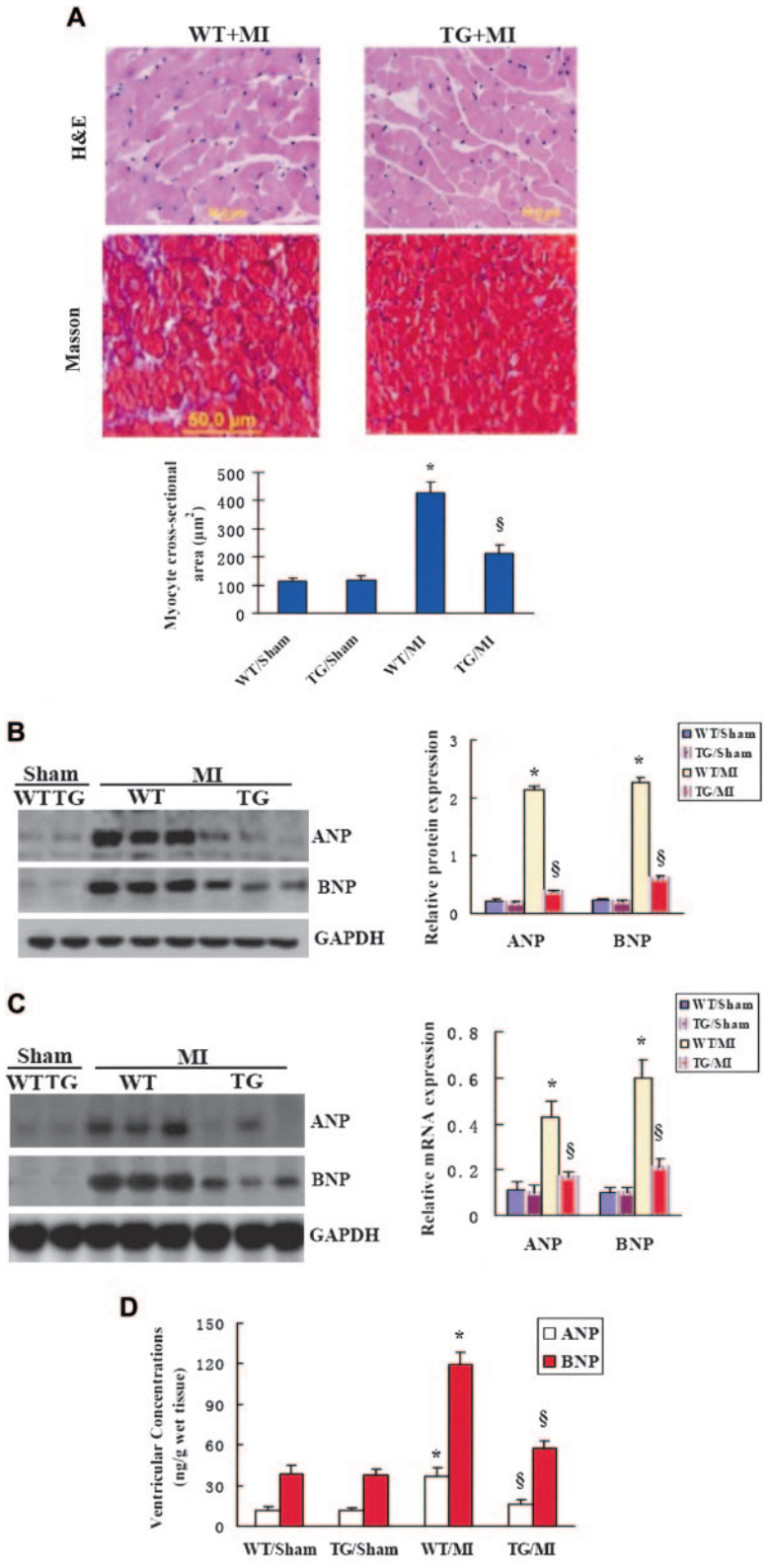

Figure 6. A20 overexpression blocks left ventricular hypertrophy induced by myocardial infarct. A, Histological sections from WT and TG mice stained with hematoxylin-eosin (top) and Masson's trichrome staining (middle) and cardiomyocyte cross-sectional area (25 sections from 4 mice per genotype; bottom). B, C, Northern and Western blots for ANP and BNP mRNA and protein on left ventricular RNA and protein from 4 groups of animals (n=6). GAPDH was used as loading control. Left, Representative blots; right, quantitative results. Densitometric analysis of 7 mice per genotype normalized on GAPDH. D, Ventricular ANP and BNP concentrations. Ventricular ANP and BNP concentrations were measured by specific radioimmunoassay from 4 groups of animals (n=6). Values are mean±SEM. *$P<0.01$ vs WT-sham values; §$P<0.01$ vs WT-MI values.

than those in sham-operated mice. Importantly, the ventricular ANP and BNP levels were markedly lower in TG-MI mice than in WT-MI mice. Consistent with ANP and BNP expression results, the ratio of heart weight to body weight was increased significantly in the WT-MI groups compared with noninfarcted controls, whereas the ratio of heart weight to body weight of TG-MI mice was significantly lower (the Table). Lung and liver weights were found to be unaltered between all groups investigated (data not shown). These results indicate that A20 efficiently blocks cardiac remodeling by modulating the expression and concentration of hypertrophy-related genes in post-MI hearts.

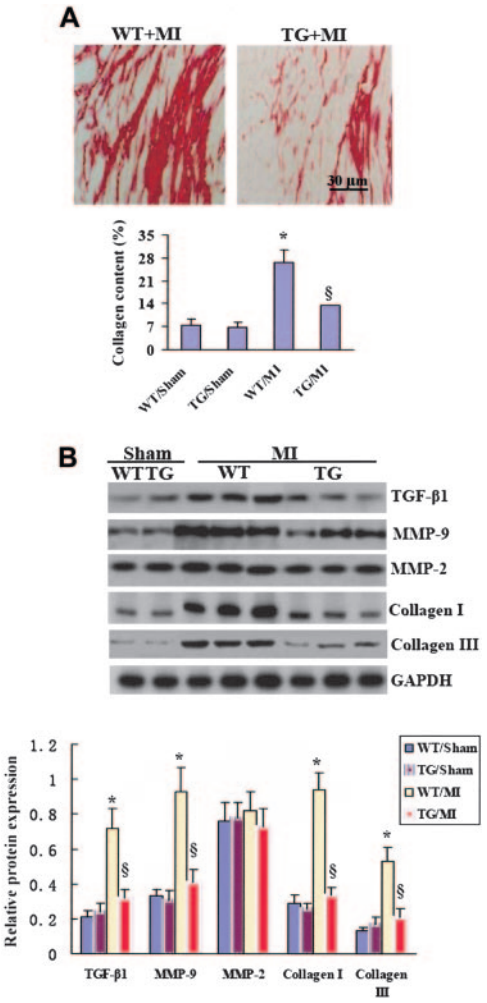

Figure 7. A20 overexpression prevents fibrotic tissue deposition induced by myocardial infarct. A, Picrosirius red staining on histological sections from WT and TG left ventricle 7 days after MI (top) and fibrotic area quantified by image-analyzing system on histological sections from 5 different hearts per genotype (10 sections per mouse; bottom). B, Western blot analysis of MMP-2, MMP-9, TGF-β1, collagen I, and collagen III from 4 groups of animals (n=6) 7 days after MI. GAPDH was used as sample loading control. Top, Representative blots; bottom, quantitative results. Values are mean±SEM. *$P<0.01$ vs WT-sham values; §$P<0.01$ vs WT-MI values.

A20 Overexpression Protects From Fibrosis in Noninfarcted Region After MI

Heart sections were stained with picrosirius red to detect fibrosis. In both groups, collagen continued to accumulate at the site of infarction 7 days after MI. In the infarct zone itself, the collagen deposition was not different from that in the 2 groups. However, increased collagen deposition was observed in WT myocardium remote from the site of infarction, including the septum, right ventricle, endocardium, and pericardium. In WT mice, multiple patchy foci of fibrosis were observed on microscopy in the remote zone, but this was conspicuously reduced in TG mice (Figure 7A). Quantitative analysis also showed increased collagen volume in the noninfarcted region ($P<0.01$) in WT mice compared with TG mice. We also focused on the synthetic processes involved in collagen turnover by examining the expression of protein encoding matrix metalloproteinase (MMP)-2, MMP-9, transforming growth factor (TGF)-β1, collagen I, and collagen III (Figure 7B), which are known to be involved in cardiac fibroblast proliferation and the biosynthesis of extracellular matrix proteins. We found that MMP-9, TGF-β1, collagen I, and collagen III expression was significantly higher in WT than TG mice after ligation, whereas there was no difference in the expression of MMP-2.

Discussion

In the present study, we have demonstrated for the first time that overexpression of A20 in the heart can achieve high levels of human A20 expression in mice and results in myocardial protection in terms of reduced infarct size and improved cardiac function after acute MI. This myocardial protective effect in A20-overexpressed hearts is associated with reduced inflammatory response, attenuated cardiomyocyte apoptosis, and impaired left ventricular remodeling. We also have shown that overexpression of A20 in our TG model results in supranormal levels of this protein in infarcted/noninfarcted myocardium. This presumably results because expression of TG A20 protein is controlled by the α-myosin heavy chain promoter, which will stabilize the level of expression even under ischemic conditions. These results suggest a potentially clinically relevant molecular therapeutic strategy in which the A20 protein can have a beneficial effect in the acute MI setting.

There is growing evidence that NF-κB plays an important role in heart diseases. However, the role of NF-κB in MI is controversial. Some studies have showed that activation of NF-κB promotes the pathogenesis of cardiac remodeling and heart failure, whereas inhibition of NF-κB or its signaling has been shown to attenuate left ventricular damage and remodeling after MI.[14–17] These findings are consistent with our current results that overexpression of A20 in the heart inhibits MI-induced NF-κB activation through blocking IKKβ and p65 activation in the myocardium. Our results indicate that blocking of NF-κB activation is functionally coupled to biological signals that lead to attenuated left ventricular damage after MI. Conversely, the results of the present study conflict with studies showing that TG mice with a defect in activation of NF-κB have increased susceptibility to tissue injury after acute MI,[18] and a study by Mustapha et al[19] demonstrated that NF-κB activation has a cardioprotective effect against hypoxia in cardiomyocytes in vitro. The reason for the discrepancy in the role of NF-κB in MI remains unclear. We postulate that it may be related to differences in experimental models (ischemia/reperfusion versus left anterior descending artery or in vivo versus in vitro), differences in the strain of mice, and differences in time after ischemia. Therefore, the findings of the present study indicate that inhibition of the activation of NF-κB, although useful for reducing the effects of an acute ischemic episode, may be detrimental in the adaptation of the heart to repetitive episodes of ischemia. Thus, further studies are needed to elucidate the specific pathophysiological conditions under which the inhibition of NF-κB activation may be useful or detrimental.

It has been reported that A20 could block inflammatory responses induced by cytokines through inhibiting NF-κB activation.[6] The postinfarction inflammatory response is important for removal of irreversibly injured cells and wound healing. However, optimal repair requires timely suppression of inflammation and containment of granulation tissue formation in the infarcted area. During the inflammatory phase, infiltration by inflammatory cells, particularly neutrophils and macrophages, is followed by removal of necrotic tissue and degradation of extracellular matrix components.[1,2] We observed remarkable neutrophil and macrophage infiltration of the infarcted heart at 7 days after MI, which made up the acute inflammatory response. Importantly, the increased infiltration by inflammatory cells was attenuated by A20 expression. Inflammatory response is mediated by proinflammatory cytokines such as TNF-α, IL-1β, IL-6, and MCP-1. These cytokines are not constitutively expressed in the normal heart. Upregulation and production of these cytokines represent an intrinsic or innate stress response against myocardial injury.[1,2] In this investigation, we also found that TNF-α, IL-1β, IL-6, and MCP-1 levels decreased noticeably in TG-MI mice compared with WT-MI mice, further indicating that A20 overexpression attenuates inflammatory response mediated by acute MI. One possible mechanism for such a protective effect is that A20 expression would directly inhibit NF-κB activation, resulting in attenuation of the inflammatory response and subsequent myocardial damage, because the expression of many cytokines, including TNF-α, IL-1β, IL-6, and MCP-1, is regulated by NF-κB activation. Each molecule has a κB-binding domain in its promoter site.

Increasing evidence shows that apoptosis of cardiomyocytes is involved in the process of myocardial damage after acute MI.[20,21] Part of the myocardial dysfunction resulting from ischemia can be attributed to apoptotic and necrotic cell death. The experimental findings here show a correlation between an increase in the frequency of apoptosis and the extent of myocardial infarct size. Accordingly, we speculate that in our model, reduced cardiac myocyte apoptosis contributed significantly to markedly decreased infarct size in TG mice compared with infarcts in WT control mice. Our results corresponding to a reduction in the number of apoptotic cells in myocardium in TG mice also support the hypothesis that after acute MI cardiomyocytes die partly by an apoptotic pathway. Furthermore, it has been demonstrated that A20 blocks apoptosis of various cells associated with blocking caspase-3, -8, and -9 activation, as well as the release of cytochrome c from mitochondria.[7] Indeed, the present study demonstrates that overexpression of A20 attenuates myocardial apoptosis after acute MI and is associated with abrogated cleavages of caspase-3 and -9, as well as abolished mitochondrial dysfunction, as demonstrated by the prevention of the release of cytochrome c and Smac/Diablo. Additionally, we found that A20 expression maintained the decreased expression of the antiapoptotic proteins survivin, bcl-2, XIAP, and cFLIP and decreased the expression of the proapoptotic proteins Fas, FasL, and Bax 7 days after MI. Involvement of these signaling molecules mediated apoptosis; thus, A20 can explain the protection from apoptosis observed in TG hearts subjected to acute MI.

Ventricular remodeling after MI is a risk factor that can lead to the development of heart failure.[22,23] In the present study, we found that 7 days after MI, there was significantly elevated ratio of heart weight to body weight and upregulation of expression and concentration of ventricular ANP and BNP, indicating that post-MI hearts were hypertrophic. A20 expression prevented post-MI hypertrophy because ANP and BNP levels were markedly decreased and hearts were of normal size. Thus, preservation of global function by human A20 overexpression appears to be able to prevent the hypertrophic changes associated with acute MI that often can lead to left ventricular remodeling and heart failure. An additional feature of left ventricular remodeling of TG mice is attenuation of fibrosis as detected by both histological analysis and gene profiling experiments. This could be ascribed to negative regulation of well-known profibrotic factors such as MMP-9, TGF-β1, collagen I, and collagen III. Accumulation of stromal tissue represents a deleterious feature of left ventricular hypertrophy affecting the viscoelastic properties of the myocardium, impairing diastolic function, and favoring the transition to heart failure. The reduced fibrosis in A20 TG infarcted left ventricles could lead to improved diastolic function. Indeed, fibrosis is only one of several determinants of diastolic function; hypertensive conditions represent another crucial factor, evoking an impairment of left ventricular diastolic function independently of their impact on cardiac hypertrophic remodeling after acute MI.

Conclusions

Data from the present study indicate that cardiac-specific overexpression of the human A20 gene preserves global cardiac function in response to acute MI and prevents left ventricular dysfunction and remodeling, which may potentially delay subsequent heart failure development. Acute MI in TG mice displays several features observed in human hearts undergoing MI such as reduced inflammation, apoptosis, left ventricular remodeling, and fibrosis. Because A20 expression decreases in infarcted heart subjected to MI, upregulation of A20 expression could represent a novel strategy to activate beneficial signaling in left ventricular dysfunction, apoptosis, and remodeling and to prevent the transition to heart failure in response to acute MI.

Acknowledgments

We wish to acknowledge Professor Xiao-Ping Yang from the Henry Ford Hospital and Professor Yong-Jian Geng from the Texas Heart Institute for their critical review of this manuscript.

Sources of Funding

This research was supported by the National Basic Research Program of China (2006CB503801 to Professor D.-P. Liu and 2005CB522507 to Professor Huang).

Disclosures

None.

References

1. Nian M, Lee P, Khaper N, Liu P. Inflammatory cytokines and postmyocardial infarction remodeling. *Circ Res*. 2004;94:1543–1553.
2. Sun M, Dawood F, Wen WH, Chen M, Dixon I, Kirshenbaum LA, Liu PP. Excessive tumor necrosis factor activation after infarction contributes

to susceptibility of myocardial rupture and left ventricular dysfunction. *Circulation*. 2004;110:3221–3228.
3. Regula KM, Kirshenbaum LA. Apoptosis of ventricular myocytes: a means to an end. *J Mol Cell Cardiol*. 2005;38:3–13.
4. Morissette MR, Rosenzweig A. Targeting survival signaling in heart failure. *Curr Opin Pharmacol*. 2005;5:165–170.
5. Heyninck K, Beyaert R. A20 inhibits NF-kappaB activation by dual ubiquitin-editing functions. *Trends Biochem Sci*. 2005;30:1–4.
6. Beyaert R, Heyninck K, Van Huffel S. A20 and A20-binding proteins as cellular inhibitors of nuclear factor-kappa B-dependent gene expression and apoptosis. *Biochem Pharmacol*. 2000;60:1143–1151.
7. Li HL, Wang AB, Zhang R, Wei YS, Chen HZ, She ZG, Huang Y, Liu DP, Liang CC. A20 inhibits oxidized low-density lipoprotein-induced apoptosis through negative Fas/Fas ligand-dependent activation of caspase-8 and mitochondrial pathways in murine RAW264.7 macrophages. *J Cell Physiol*. 2006;208:307–318.
8. Cook SA, Novikov MS, Ahn Y, Matsui T, Rosenzweig A. A20 is dynamically regulated in the heart and inhibits the hypertrophic response. *Circulation*. 2003;108:664–667.
9. Thiemermann C. Inhibition of the activation of nuclear factor kappa B to reduce myocardial reperfusion injury and infarct size. *Cardiovasc Res*. 2004;63:8–10.
10. Lochard N, Thibault G, Silversides DW, Touyz RM, Reudelhuber TL. Chronic production of angiotensin IV in the brain leads to hypertension that is reversible with an angiotensin II AT1 receptor antagonist. *Circ Res*. 2004;94:1451–1457.
11. Ma XL, Yue TL, Lopez BL, Barone FC, Christopher TA, Ruffolo RR Jr, Feuerstein GZ. Carvedilol, a new beta adrenoreceptor blocker and free radical scavenger, attenuates myocardial ischemia-reperfusion injury in hypercholesterolemic rabbits. *J Pharmacol Exp Ther*. 1996;277:128–136.
12. Izumi T, Saito Y, Fujiwara H, Garbers DL, Mochizuki S, Nakao K. Blockade of the natriuretic peptide receptor guanylyl cyclase-A inhibits NF-kappaB activation and alleviates myocardial ischemia/reperfusion injury. *J Clin Invest*. 2001;108:203–213.
13. Niu J, Azfer A, Deucher MF, Goldschmidt-Clermont PJ, Kolattukudy PE. Targeted cardiac expression of soluble Fas prevents the development of heart failure in mice with cardiac-specific expression of MCP-1. *J Mol Cell Cardiol*. 2006;40:810–820.
14. Morishita R, Sugimoto T, Sawa Y, Ogihara T. In vivo transfection of cis element "decoy" against NF-KB binding site prevents myocardial infarction. *Nat Med*. 1997;3:894–899.
15. Kawano S, Kubota T, Monden Y, Tsutsumi T, Inoue T, Kawamura N, Tsutsui H, Sunagawa K. Blockade of NF-kappaB improves cardiac function and survival after myocardial infarction. *Am J Physiol Heart Circ Physiol*. 2006;291:H1337–H1344.
16. Frantz S, Hu K, Bayer B, Gerondakis S, Strotmann J, Adamek A, Ertl G, Bauersachs J. Absence of NF-kappaB subunit p50 improves heart failure after myocardial infarction. *FASEB J*. 2006;20:1918–1920.
17. Baud V, Karin M. Signal transduction by tumor necrosis factor and its relatives. *Trends Cell Biol*. 2001;11:372–377.
18. Misra A, Haudek SB, Knuefermann P, Vallejo JG, Chen ZJ, Michael LH, Sivasubramanian N, Olson EN, Entman ML, Mann DL. Nuclear factor-kappaB protects the adult cardiac myocyte against ischemia-induced apoptosis in a murine model of acute myocardial infarction. *Circulation*. 2003;108:3075–3078.
19. Mustapha S, Kirshner A, De Moissac D, Kirshenbaum LA. A direct requirement of nuclear factor-kappa B for suppression of apoptosis in ventricular myocytes. *Am J Physiol Heart Circ Physiol*. 2000;279:H939–H945.
20. Sabri A, Steinberg SF. Protein kinase C isoform-selective signals that lead to cardiac hypertrophy and the progression of heart failure. *Mol Cell Biochem*. 2003;251:97–101.
21. Honda HM, Korge P, Weiss JN. Mitochondria and ischemia/reperfusion injury. *Ann N Y Acad Sci*. 2005;1047:248–258.
22. Weiss JN, Korge P, Honda HM, Ping P. Role of the mitochondrial permeability transition in myocardial disease. *Circ Res*. 2003;93:292–301.
23. Molkentin JD. Calcineurin, mitochondrial membrane potential, and cardiomyocyte apoptosis. *Circ Res*. 2001;88:1220–1222.

CLINICAL PERSPECTIVE

Cardiovascular disease remains the major cause of morbidity and mortality in the Western world, and the incidence of heart failure is rapidly increasing, mostly as a result of the reduction in mortality after acute myocardial infarction. After the acute phase of myocardial infarction, a chronic phase of ventricular remodeling occurs. This phase is maladaptive and associated with persistent cardiomyocyte apoptosis, inflammation, fibrosis, and hypertrophy, which contribute to the development of depressed cardiac function, clinical heart failure, and increased mortality. Intervention to minimize these progressive changes is highly desirable to reduce the incidence and severity of the congestive heart failure that may develop after myocardial infarction. Therefore, it is of critical importance for us to better understand the molecular basis of heart failure, which could allow us to develop more specific and more effective therapies. One way to achieve successful attenuation of heart failure is to overexpress some proteins in the heart that are usually protective of cardiac inflammation, apoptosis, fibrosis, and hypertrophy. In this regard, A20 has become a research focus because of its antiapoptotic, antiinflammatory, and antihypertrophic properties. In the present study, we provide evidence for the protective role of A20 in heart failure through the use of biomechanical and ischemic heart failure models in cardiac-specific A20 transgenic mice. Therapies designed to overexpress A20 in the heart might be beneficial in preventing clinical heart failure.